

Genomic Sequence Analysis of the Mouse *Naip* Gene Array

Matthew G. Endrizzi,^{2,4} Vey Hadinoto,² Joseph D. Growney,² Webb Miller,³ and William F. Dietrich^{1,2,5}

¹Howard Hughes Medical Institute and ²Department of Genetics, Harvard Medical School, Boston, Massachusetts 02115 USA; ³Department of Computer Science and Engineering, Pennsylvania State University, University Park, Pennsylvania 16802 USA

A mouse locus called *Lgn1* determines differences in macrophage permissiveness for the intracellular replication of *Legionella pneumophila*. The only regional candidate genes for this phenotype difference lie within a cluster of closely linked paralogs of the Neuronal Apoptosis Inhibitory Protein (*Naip*) gene. Previous genetic and physical mapping of the *Lgn1* phenotype narrowed it to an interval containing only *Naip2* and *Naip5*, suggesting that there is not complete functional overlap among the mouse *Naip* loci. In order to gather more information about polymorphisms among the *Naip* genes of the I29 mouse haplotype, we have determined the genomic sequence of a substantial portion of the I29 *Naip* gene array. We have constructed an evolutionary model for the expansion of the *Naip* gene array from a single progenitor *Naip* gene. This model predicts the presence of two distinct families of *Naip* paralogs: *Naip1/2/3* and *Naip4/5/6/7*. Unlike the divergences among all the other *Naip* paralogs, the splits among *Naip4*, *Naip5*, *Naip6*, and *Naip7* occurred relatively recently. The high degree of sequence conservation within the *Naip4/5/6/7* family increases the likelihood of functional overlap among these genes.

[The sequence data described in this paper have been submitted to the GenBank data library under accession nos. AF242431-AF242435.]

Macrophages isolated from C57BL/6J and A/J mice exhibit differences in permissiveness for intracellular replication of *L. pneumophila* (Yamamoto et al. 1988). This phenotype difference segregates as a single-gene trait in crosses between C57BL/6J and A/J and maps to a locus on distal chromosome 13 (Yamamoto et al. 1991; Yoshida et al. 1991; Dietrich et al. 1995; Beckers et al. 1995). Detailed physical mapping of this locus, called *Lgn1*, reveals that it contains a series of 50 to 80 kb highly homologous direct repeats and that a cluster of *Naip* gene paralogs map inside these direct repeats (Scharf et al. 1996; Growney et al. 2000).

The region of the human genome that is orthologous to the mouse *Lgn1* region also contains a series of highly homologous repeated segments. The human spinal muscular atrophy (*SMA*) region has what appears to be an inverted duplication of some 500 kb (Lefebvre et al. 1995). This amplified genomic segment contains several transcriptionally active genes, including copies of survival motor neuron (*SMN*); *NAIP*; general transcription factor II H, polypeptide 2 (*GTF2H2*); and small EDRK-rich factor 1 (*SERF1*) (reviewed by Growney et al. 2000). However, the only gene in common between the amplified segments from the mouse and human *Lgn1/SMA* intervals is *Naip/NAIP* (Growney et al. 2000).

The fact that the mouse and human *Lgn1/SMA* regions both have divergently organized sets of closely

linked repeats indicates that these amplified segments originated independently in the mouse and human lineages. This observation begs the question of whether the amplification of *Naip/NAIP* in either mouse or human has any functional significance. Although most of the mouse *Naip* paralogs are transcriptionally active and encode similar but not identical proteins, it is not known whether these transcripts provide redundant or diverse functions (Huang et al. 1999). These questions about the functionality of the mouse *Naip* loci are important to the identification of the *Lgn1* mutation because the current critical interval for the *Lgn1* phenotype contains two different transcriptionally active *Naip* genes (*Naip2* and *Naip5*) (Growney and Dietrich 2000; Huang et al. 1999).

Mapping and sequence analysis of the mouse *Lgn1* interval suggests that the *Naip* genes have arisen through a series of several distinct amplification events emanating from a single ancestral *Naip*. This model of the origins of the mouse *Naip* array relies heavily on the sequences (Fig. 1A) of a single exon from the clustered *Naip* paralogs to build a phylogenetic tree (Growney et al. 2000). A more rigorous basis for determining the relationships of the mouse *Naip* genes would be to compare their entire genomic sequences.

In this paper, we report the complete annotated sequence of 26f17, a 220-kb bacterial artificial chromosome (BAC) clone that contains the three *Naip* genes on the centromere-distal side of the array in the I29 haplotype (*Naip1*, *Naip3*, and *Naip6*) (Fig 1A; Growney et al. 2000). In addition, we present three large annotated fragments of genomic sequence from 9045, a 75-

⁴Present address: Whitehead Institute/MIT Center for Genome Research, Cambridge, MA 02142.

⁵Corresponding author.

E-MAIL dietrich@rascal.med.harvard.edu; FAX (617) 432-3993.

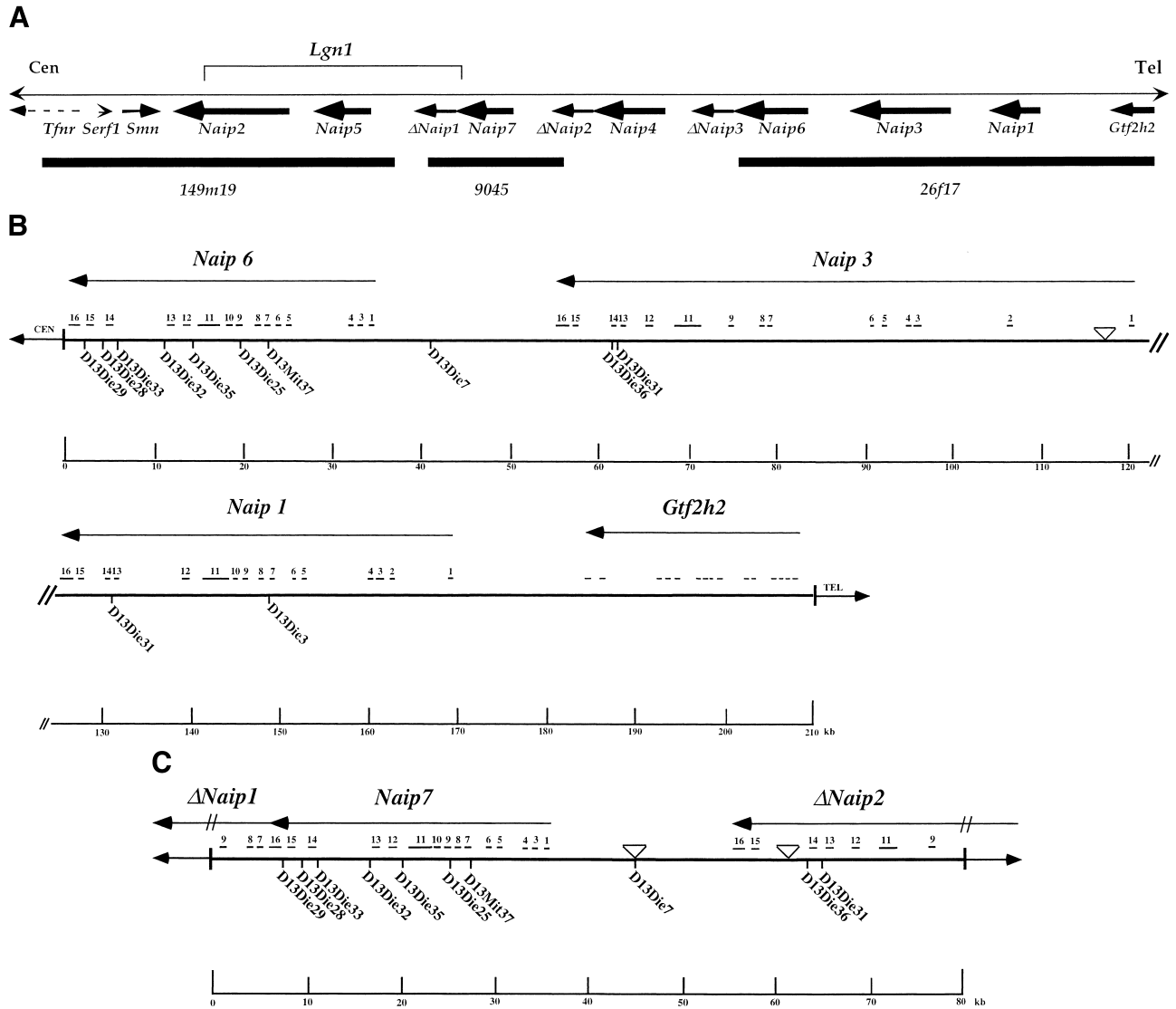


Figure 1 Map of the 129 mouse *Naip* array and annotation of the genomic sequences. (A) The map of the 129 mouse *Naip* array that was described previously in Growney et al. (2000) is indicated. The named arrows show the position and orientation of the *Naip* gene loci. The Δ *Naip* regions are pseudogenes that have been deleted for several of the 5' terminal exons. The current critical interval for *Lgn1* is indicated above the map (Growney and Dietrich, 2000). The positions of genomic clones with sequence reported in this work (9045 and 26f17) or elsewhere (149m19, Endrizzi et al. 1999) are indicated by bold lines beneath the gene map. The positions of other nearby genes are indicated to provide context for the map. For Fig. 1B,C, the identification and annotation of *Naip* gene sequences were obtained through simple alignments of known *Naip* cDNA sequences to the genomic fragments (see Methods). The sequences were also analyzed using Genotator/Genotator Browser (see Methods). The relative orientations of named transcription units, gene exons, and markers in each clone are shown in these figures. The scale at the bottom is in kb. The arrows represent the direction of transcription of the genes and the position and size of exons from within the genes are shown by the small numbered lines, except in the case of *Gtf2h2*, which has its coding exons indicated, but its 5' and 3' untranslated-region sequences in the mouse are unknown. (B) Annotation of 26f17 (AF242431 and AF242432). The triangle indicates the position of an approximately 7-bp gap in the sequence that cannot be determined with certainty. (C) Annotation of 9045 (AF242433-AF242435). The triangles indicate the positions of two small gaps (each are ~500 bp) in the sequence.

kb P1 clone mapping to the central portion of the 129 *Naip* array (Fig 1A; Growney et al. 2000). Our analysis of these genomic sequences has provided additional markers to refine the map of the *Lgn1* interval (Growney and Dietrich 2000) and allowed us to refine the previously reported model of the origins of the mouse *Naip* array.

RESULTS

Genomic Sequence Determination

The 220-kb BAC clone 26f17 was roughly mapped to the distal side of the *Lgn1* region by others (Diez et al. 1997). Subsequent precise mapping of the clone identified it as an ideal template for sequencing the *Lgn1*

interval because it covered a large extent of the distal side of the *Naip* gene array (Fig 1A; Growney et al. 2000). Our prior map information about this clone suggested that it was likely to contain multiple copies of *Naip* gene sequences; so we used a tiered strategy for the sequence assembly (see Methods; Endrizzi et al. 1999).

The final sequence assembly of this clone consists of two contiguous sequences covering 117,791 bp and 90,650 bp (GenBank accession nos. AF242431 and AF242432). We could not complete the sequence across the remaining gap with certainty because it was composed of a 300-bp simple sequence repeat. We were able to link the two contiguous sequences using the polymerase chain reaction (PCR), and our estimate of the total sequence length (208,448 bp) suggests an extremely small gap of only 7 bp (Fig. 1B). The two consensus sequences were derived from 3960 sequencing reactions, with every base in the consensus representing data from at least one sequencing reaction on each strand. The average per-base sequencing redundancy is over fivefold. The sequence assembly was analyzed extensively for consistency with known restriction digest and PCR amplification patterns from clone and genomic DNA, indicating that the sequence represents both the clone and the genomic structure with fidelity (data not shown).

P1 clone 9045 was identified by us several years ago and subsequently mapped with precision into the center of the *Naip* array (Fig. 1A) in 129 (Scharf et al. 1996; Growney et al. 2000). We chose to sequence this clone because of its position in the center of the *Naip* array because it could reveal significant discrepancies from our model of the origin of this repeat. We used a similar strategy for sequence assembly as we did for 26f17.

The final sequence assemblies for 9045 consist of three contiguous sequences totaling 72,460 bp (GenBank Accession nos. AF242433–AF242435). The holes in the sequence represent areas that are difficult to sequence because they contain microsatellite sequences. However, we measured the size of the remaining gaps in the sequence using PCR and found them to be quite small (Fig. 1C). The three consensus sequences were derived from a total of 1355 sequencing reactions and as with 26f17, every base in the sequence represents data from each strand. The average per-base sequencing redundancy is approximately fivefold. The total size of the known sequence and our estimates of the gap sizes are in accordance with our estimates of the size of 9045 from *NotI* digestion and pulsed field gel analysis (data not shown).

Discovery and Annotation of Genes in 26f17 and 9045

We have used several methods to discover and annotate genes in our new genomic sequences. Because we

knew that the clones were going to contain *Naip* gene loci, the first—and most straightforward—annotation relied on aligning known *Naip* cDNA sequences to the clones (Fig. 1).

Naip Loci in 26f17:

Naip1. The distal-most *Naip* gene in the cluster, *Naip1*, spans 45 kb and has 16 exons, including an exon 2 in its 5' untranslated region (UTR), which is a sequence found only in *Naip1*, *Naip3*, and *Naip2* (see below; Endrizzi et al. 1999). This gene is transcriptionally active but has been genetically excluded from the *Lgn1* interval (Yaraghi et al. 1998; Huang et al. 1999; Growney et al. 2000).

Naip3. *Naip3*, which spans approximately 65 kb, is likely to be a nonfunctional gene sequence. We have never isolated a cDNA corresponding to transcripts from this locus, and the genomic sequence shows that the region corresponding to exon 10 of this gene is completely absent, which likely creates a frameshift if exon 9 is spliced directly to exon 11 (Huang et al. 1999). As suggested previously, *Naip3* is likely to be the direct progenitor of the so-called fragmentary $\Delta Naip$ sequences (see below; Growney and Dietrich 2000).

Naip6. As has been seen with the genomic sequence of *Naip5*, this gene sequence, which spans approximately 35 kb, has only 15 exons and contains a number of polymorphic marker sequences that characterize members of the central *Naip* repeat (Endrizzi et al. 1999; Growney et al. 2000). This gene is likely to be transcriptionally active because cDNAs from close relatives of this locus have been isolated (Huang et al. 1999). The 3' UTR of these cDNAs contain unspliced exons from an adjacent $\Delta Naip$ locus. Unfortunately, our sequence of 26f17 does not extend into the region where these $\Delta Naips$ should reside. Nevertheless, a marker called D13Die30, that specifically amplifies $\Delta Naips$ from genomic DNA, maps proximally to *Naip6* (Growney et al. 2000). Furthermore, we have determined the sequences of $\Delta Naip$ loci from our assembly of 9045 (see below). The only ortholog of *Naip6* contained in the C57BL/6J genome has been excluded from the *Lgn1* interval (Growney and Dietrich 2000).

Naip Loci in 9045:

Naip7. *Naip7*, which spans approximately 30 kb, has many similarities to *Naip5* and *Naip6*, including the number of exons and the presence of repeated microsatellite markers characteristic of the central *Naip* array. In addition, it is similar to *Naip6* but diverges from *Naip5* in that it has a $\Delta Naip$ juxtaposed at its 3' end. As we noted for *Naip6*, it is possible that this gene is transcriptionally active, since cDNAs from a relative of this locus in another mouse strain have been isolated (Huang et al. 1999).

$\Delta Naips$. We have sequenced portions of two differ-

ent $\Delta Naip$ loci in 9045. From these two partial $\Delta Naip$ sequences, we discerned two important features. First, the $\Delta Naip$ loci, which span approximately 20 kb, begin with an exon 7 that is juxtaposed extremely close to the exon 16 of the adjacent *Naip*. Second, the marker content of the $\Delta Naip$ loci are similar to that of *Naip3*, as can be seen by the presence of D13Die36, the size of its intron 13, and the absence of an exon 10. All these data point strongly to the possibility that $\Delta Naips$ are recently diverged relatives of *Naip3*. However, one significant difference between *Naip3* and the $\Delta Naips$ is seen in exon 11, which is present in only a fragmentary form in the $\Delta Naips$.

In addition to aligning our sequences with cDNAs known to map into the interval, we subjected them to a series of homology searches and gene prediction programs using the Genotator and Genotator-Browser packages (Harris 1997). We identified only one other gene in our sequences using this method. Consistent with prior data, we found sequences from 26f17 having significant BLAST homologies to human *GTF2H2* sequences (Growney et al. 2000). Because the cDNA sequence for the mouse ortholog has not been determined, we aligned the human cDNA to 26f17 and de-

termined the intron-exon structure of the coding portion of the mouse *Gtf2h2* gene, but we could not definitively identify the 5' and 3' UTR sequences. For that reason, we have not numbered the exons of *Gtf2h2* that are depicted in Figure 1.

Alignments of Mouse *Naip* Sequences

Given the sequence relatedness of the mouse *Naip* gene loci, it is likely that they all share a single common progenitor. We have done alignments of the known mouse *Naip* sequences in order to shed some light about the nature of the events that have taken place since the divergence from a single *Naip* gene (see Methods). The data from these alignments is presented in Figure 2 and Table 1.

Inspection of Figure 2A, in which the alignments of the *Naip* genes are represented as a Percent Identity Plot (PIP), shows that *Naip5*, *Naip6*, and *Naip7* are extremely closely related to each other, confirming either that they are the result of recent gene duplications or that they are subject to homogenization via gene conversion. Similarly, *Naip1*, *Naip2*, and *Naip3* share extensive alignments with each other, indicating that they are closely related (Fig. 2A; Table 1). The amount

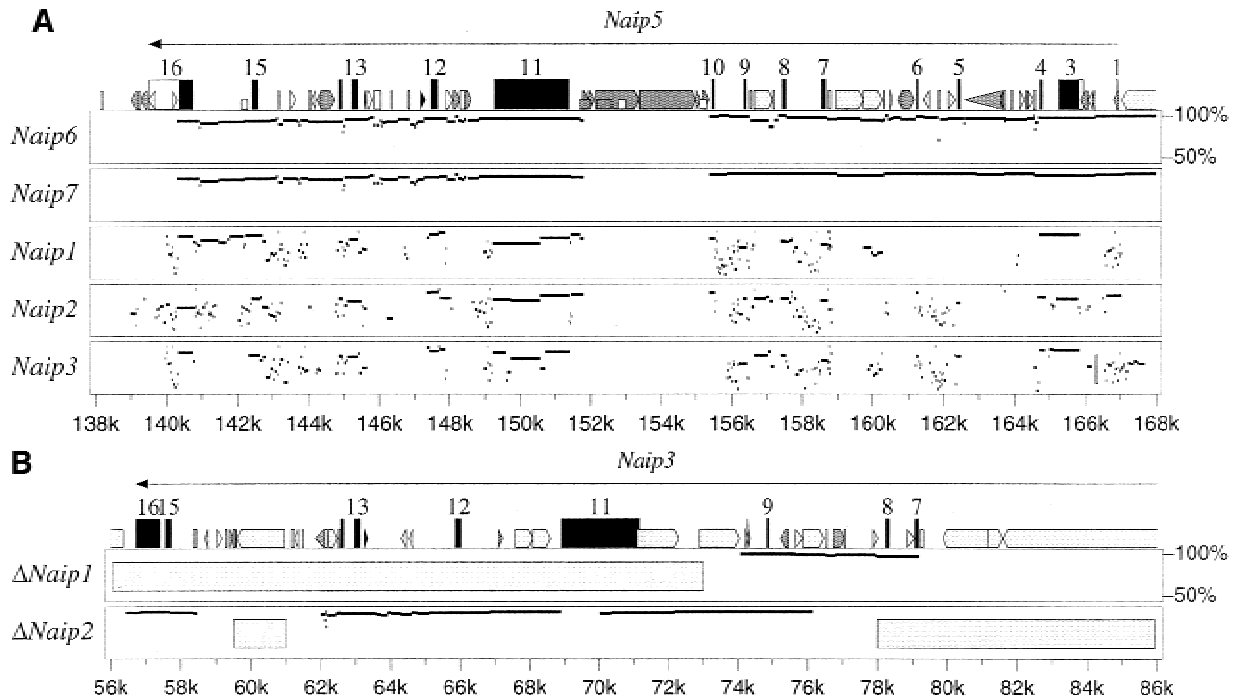


Figure 2 Percent Identity Plot (PIP) Analysis of *Naip* Genomic Sequences. The alignments have been generated and drawn as described in Methods. The figure indicates regions for which there are alignments having >50% identity. Before alignment, the genomic sequences were masked by RepeatMasker. Interspersed repeats in the mouse sequence are indicated as follows: (white pointed box) L1; (light gray box) SINE other than MIR; (black box) MIR or LINE2; (dark gray box) all others. Other elements in the sequence are indicated as follows: (arrows), positions and directions of transcription of known genes in the query sequence; (numbered black rectangles) positions of exons within the transcription units; (short gray rectangles), position of CpG islands. The figure shows several PIPs between mouse *Naip* genes. (A) Comparison of the *Naip5* to all the other sequenced *Naips*, showing the existence of two distinct families of gene loci: *Naip1/2/3* and *Naip4/5/6/7*. (B) Comparison of *Naip3* with the $\Delta Naip$ loci. The elongated gray boxes inside the PIP panels indicate regions in which a comparison between the two sequences is not possible because one of the sequences ends.

Downloaded from by guest on March 10, 2025. Copyright 2000

Table 1. Comparison of Alignments of Mouse *Naip* Paralogs^a

	<i>Naip1</i> ^b		<i>Naip2</i> ^c		<i>Naip3</i> ^d		<i>Naip5</i> ^e		<i>Naip6</i> ^f		<i>Naip7</i> ^g	
	align	ident										
<i>Naip1</i> ^b	—	—	36	78	46	82	48	80	37	79	45	77
<i>Naip2</i> ^c	46	81	—	—	34	81	49	75	36	80	44	73
<i>Naip3</i> ^d	67	80	37	79	—	—	46	72	46	78	34	85
<i>Naip5</i> ^e	27	80	21	76	17	77	—	—	63	95	78	94
<i>Naip6</i> ^f	29	80	22	77	24	80	86	94	—	—	100	97
<i>Naip7</i> ^g	28	80	21	75	15	85	86	96	82	98	—	—

^aThe genomic sequence for each *Naip* gene locus was aligned with each other *Naip* locus (see Methods). The similarities between these alignments are expressed in terms of the percentage of the gene named in the column head that appears in a local alignment with the gene named in the row head (column labeled “align”) and of the percentage of sequence identity within those local alignments (column labeled “ident”). Because of the differences in the overall length of the different *Naip* genes, it is important for the reader to confine their comparisons to looking for trends within a column. In this way, one can see the relationships among the different families of *Naip* genes. For example, by looking in the *Naip1* column, one can see that it most resembles *Naip3*, because of the extensive proportion of *Naip1* that aligns with *Naip3*. On this basis, one can also see that *Naip1* is more closely related to *Naip2* and *Naip3* than it is to *Naip5*, *Naip6*, or *Naip7*. The parameters used in generating the local alignments prohibit little variation in the percent identity of the alignments. An exception to this is seen in the homologies among the *Naip5/6/7* family, in which the percent identities typically exceed 90%.

^bBases 6546-51581 of GenBank no. AF242432.

^cBases 68968-128492 of GenBank no. AF131205.

^dBases 56706-117791 of GenBank no. AF242431 and 1-2335 of GenBank no. AF242432.

^eBases 140365-165807 of GenBank no. AF131205.

^fBases 22-34589 of GenBank no. AF242431.

^gBases 5565-34032 of GenBank no. AF242433.

of alignment and levels of homology among the two groups of paralogs suggest an early duplication of an ancestral *Naip*, leading to the progenitors of what can be called the *Naip1/2/3* and *Naip4/5/6/7* families (Fig. 2A; Table 1). Even though we do not have genomic sequence for *Naip4*, we have included it in the *Naip4/5/6/7* group based on prior published data demonstrating a high degree of similarity in marker content (Growney et al. 2000).

Although the amplification of the *Naip5*, *Naip6*, and *Naip7* gene loci seems to be a recent event (as demonstrated by their extremely high level of sequence conservation and their virtually complete alignment that is broken only by the insertion of interspersed repeat elements), the amplification and divergence of the *Naip1*, *Naip2*, and *Naip3* loci appears to have happened longer ago (as suggested by their lower level of sequence conservation and alignment). Our analysis of the overall conservation of alignments between the *Naip1/2/3* sequences, suggests that *Naip2* diverged from *Naip1/3* before a more recent split between *Naip1* and *Naip3* (Fig. 2A; Table 1).

Our alignments of the *Naip3* locus confirmed our suspicion that the $\Delta Naip$ loci are extremely close relatives of *Naip3*—No other *Naip* locus exhibited such extensive alignment and high level of sequence identity (Fig. 2B). This suggests that the formation of the $\Delta Naip$ loci occurred after the split between *Naip1* and *Naip3*. Similarly, because the structure of the $\Delta Naip$ loci are identical throughout the central *Naip* repeat, the for-

mation of the $\Delta Naip$ loci likely occurred before or as part of the amplifications that created *Naip5*, *Naip6*, and *Naip7*. We summarized our interpretation of these data in a model of expansion of the mouse *Naip* array in Figure 3.

DISCUSSION

The arrangement of highly related genes in closely linked clusters is commonly seen in mammalian genomes. Broadly speaking, these arrays are of two types: those whose members have acquired important divergent functions and those whose members are redundant in function. Examples of closely linked gene families whose members have divergences in function are seen in the cases of the color-vision genes and the beta-globins (Nathans et al. 1986; Yokoyama et al. 1993; Fritsch et al. 1980; Hardies et al. 1984). Similarly, there are examples of the occurrence of closely linked gene copies that are redundant in function, such as is seen in the observed amplification of ribosomal RNA genes in various organisms and in the cellular acquisition of resistance to chemotherapeutic agents (Nath and Bollon 1977; Raymond et al. 1990).

The mouse *Naip* gene cluster is interesting because we currently do not know if it represents an example of functional diversity, functional redundancy having some important phenotypic consequence or even perhaps a fixation of an amplification that has no functional impact on the organism. Furthermore, the mouse *Naip* cluster is interesting because one of the

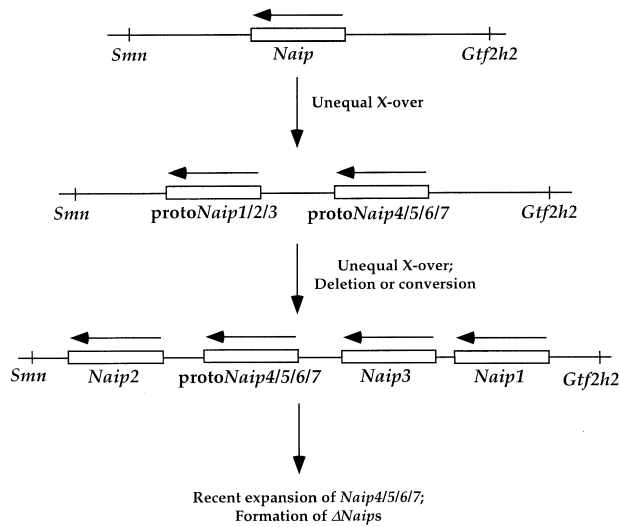


Figure 3 Model of the Origin of the *Naip* Gene Array in 129. The essential features of this model are as follows. First, the single ancestral *Naip* gene became duplicated. This duplication may have occurred due to an unequal crossing over event between different copies of an interspersed repetitive element. This original duplication event is strongly suggested by the sequence similarity profiles between different *Naip* genes and represents the ancient split between the *Naip*1/2/3 and the *Naip*4/5/6/7 families. Second, the proto *Naip*4/5/6/7 locus becomes flanked by *Naip*2 on its centromere proximal side and by *Naip*1 and *Naip*3 on its centromere distal side. The mechanisms whereby this occurred are obscure, but the possibilities include additional duplications of the array via unequal crossing over and deletion or gene conversion of some of the resulting distal loci. Third, the origin of the central portion of the *Naip* array, including the Δ *Naip* loci, occurred much more recently; a model for this is described elsewhere (Growney et al. 2000).

members of this family must play an important role in determining the permissiveness of macrophages to the intracellular replication of *L. pneumophila* (Growney et al. 2000). In light of these unanswered questions, we have determined the genomic sequence of substantial portions of the mouse *Naip* gene array from 129 in an attempt to measure the relatedness of all the *Naip* genes.

In our analyses of these genomic sequences, we have definitively ascertained that the mouse *Naip* gene cluster can be divided into two families: the *Naip*1/2/3 family and the *Naip*4/5/6/7 family. The sequence relations of the members of these two families suggests that the *Naip*4/5/6/7 family members have diverged from each other relatively recently and may, as a consequence, share more functional relatedness than the members of the *Naip*1/2/3 family. However, since the molecular functions of each of the mouse *Naip* paralogs have been incompletely described, the sequence data alone cannot be used to make definitive statements about potential similarities or differences in function.

Nevertheless, two lines of additional evidence indicate that the functions of the different mouse *Naip* paralogs can be separated from each other. First, the

recent report of a knockout of the *Naip*1 gene illustrates a function of this gene in neuronal survival during physiological insult (Holcik et al. 2000). It is unclear whether the inability of the other *Naip* gene paralogs to compensate for the loss of *Naip*1 function has to do with differences in the molecular activity of the *Naip* proteins, with an overall diminishment of *Naip* function or with some tissue specificity in expression of the *Naip* paralogs.

The second line of evidence in favor of divergent functions of the mouse *Naip* genes comes from our knowledge of the genetic map position of the mouse *Legionella* susceptibility locus (*Lgn1*). *Lgn1* has been mapped to an interval that only includes *Naip*2 and *Naip*5, suggesting that the other *Naip* paralogs cannot compensate for a mutation in one of these genes (Growney and Dietrich 2000). Unfortunately, based on the current information, it is impossible to tell which of the two remaining candidates is responsible for the *Lgn1* phenotype.

Remaining unanswered is the broader question of whether the differences in *Naip*/*NAIP* gene content in the mouse and human genomes indicate differences in gene function between the two species. Based on previously published data, it seems that there is only a single human *NAIP* locus that produces an intact, translationally competent transcript (Roy et al. 1995). Unfortunately, critical pieces of information about the human region are missing or unclear.

For example, while it is well documented that differences in the structure of the SMA region exist among human individuals, only a few haplotypes have been mapped in detail (Lefebvre et al. 1995; Roy et al. 1995). The situation is further complicated by the fact that human genomic libraries consist of clones from at least two different haplotypes. Given that assembling a sensible map of the mouse *Lgn1* region was extremely difficult in a situation where only one haplotype was being assembled, the complexity of making a consistent human map from mixed haplotype libraries presents even more of a challenge (Growney et al. 2000; Growney and Dietrich 2000). Indeed, it remains possible that there is more variation in the number of functional *NAIP* sequences among human individuals than had been previously believed because of the technical difficulties involved in mapping the region. In addition, the extent of human variation in permissiveness to *Legionella* replication is currently unknown, making any cross-species structure-function comparisons impossible.

Because of the complexities of mapping and studying the human interval, it seems likely that the mouse will serve as a springboard for progress into understanding the origins and functional diversity of the *Naip* array. Not only can the structures of the *Naip* array be well described in inbred mouse strains, but we

and others are making significant progress in elucidating the functional roles of these genes in a variety of processes. With regard to identifying the *Lgn1* gene, it is most likely that further comparative sequencing in search of causative mutations in *Naip2* or *Naip5* and/or attempts to complement the phenotype will resolve the matter. These experiments are currently underway in our laboratory.

METHODS

Sequencing

The strategy used for determining the sequence of clones that contain multiple copies of highly related regions was described extensively elsewhere (Endrizzi et al. 1999). Here, we briefly describe the technical aspects to the sequencing.

BAC DNA Isolation

We isolated BAC (26f17) DNA from 100 ml overnight cultures (LB with 12.5 µg/ml chloramphenicol) following Research Genetics' BAC miniprep protocol. We isolated P1 (9045) DNA from 500 ml overnight cultures (LB with 50 µg/ml kanamycin) using Qiagen's Large Construct Kit.

Library Construction

We sheared 10 µg of BAC DNA in 50 µl of 1X Mung Bean buffer (New England Biolabs) using a sonicator and made the fragment ends blunt by incubating 0.5 µl of Mung Bean nuclease with the sheared DNA for 30 min at 30° C. We ran total DNA through a 1% low-melt agarose gel (FMC) in 1X TAE buffer at 1.5 V/cm for 16 hr alongside a 1 kb DNA ladder (GIBCO). We excised DNA fragments in the range of 3.5 to 4.5 kb, extracted with buffer-saturated phenol and after ethanol precipitation, resuspended in 20 µl dH₂O. We quantified the size-selected DNA against a low mass ladder (GIBCO) using an agarose gel. We ligated 150 ng of blunt-end murine DNA to 50 ng of dephosphorylated, *Sma*I blunt-cut pUC18 vector (Pharmacia) at 14° C for 16 hr and used 2 µl of the ligation reaction for transforming DH5α ultracompetent *Escherichia coli* cells (GIBCO).

Sequencing Template Preparation

We picked colonies by hand and inoculated in 96 deep-well plates containing 1.25 ml of TB plus ampicillin (50 µg/ml final). Cultures grew at 37° C for 20 hr while shaking at 225 rpm. We isolated plasmids using a 96-well alkali lysis protocol (Edge Biosystems) and resuspended in 30 µl of 1 mM Tris-Cl.

Sequencing Reactions

We sequenced 500 ng of template using ABI Big Dye terminator chemistry (Perkin Elmer) according to the manufacturer's specifications. We performed the reaction in an MJ Research thermal cycler (PTC-225). We purified reactions with 96-well filter plates (Edge), dried samples in a Speedvac evaporator, and stored the samples at -20° C until resuspending in loading buffer. We used both an ABI 377 and an ABI 3700 for detection. We extracted DNA sequences using Bass, Grace, and Trout (Whitehead/MIT) for ABI 377 data and ABI Data Collection software (Perkin Elmer) for ABI 3700 data.

Assembly

We imported approximately 4X coverage for each genomic clone in sequence reads from both ends of 4-kb subclones into

a Gap4 database (Staden 1996). We used an initial threshold of 5% mismatch for automated assembly. We then manually removed and reassembled misaligned reads based on our observations of consistent sequence polymorphisms with the consensus. Ultimately, this low-level sequence coverage of the clones yielded a manageable number of contiguous sequences that were ordered and oriented by linking subclones (Chen et al. 1993). We isolated the inserts of these subclones and sequenced sheared, cloned 500-bp fragments to obtain sequence coverage of the gaps.

Long PCR to Obtain Gap-spanning Fragments

We chose primers for long PCR using Primer 0.5 on consensus sequence from the ends of assembled contiguous sequences for which we had no linking subclones (Lincoln et al. 1991). We designed long PCR reactions to cover all possible orders and orientations of contiguous sequences. We repeated three reactions for each positive PCR product to eliminate early-round mutations introduced in any one reaction and pooled products together for either direct sequencing or library construction.

Confirmation of Sequence

To check the sequence assembly for errors, we compared the restriction digest pattern of each clone to a virtual digest of the consensus sequence. In all cases, the predictions were consistent with the digest pattern (data not shown).

Analysis and Annotation of the Sequence

Alignment with Known cDNA Sequences

We assembled sequences of *Naip* cDNAs (Huang et al. 1999) to genomic consensus sequence using Sequencher 3.0.

Genotator

After the assembly was complete, we utilized Genotator/Genotator Browser (Harris 1997) to annotate the final sequence with BLAST homologies to the expressed-sequence-tag and GENPEPT databases, open reading frames, and exons predicted by the programs Genie, GENSCAN, GRAIL, and GeneFinder (Kulp et al. 1996; Burge and Karlin 1997; Uberbacher and Mural 1991; Solovyev et al. 1994). See the paper by Endrizzi et al. (1999) for more details.

Alignments with Mouse Paralogous Sequences

Sequences were aligned using a program called Blastz (Schwartz et al. 2000), which can be run on user-supplied data at <http://bio.cse.psu.edu/>. We aligned unmasked sequences using the default alignment scores (match, 1; mismatch, -1; gap of length k , $-6-0.2k$) and the Chaining option, which forces aligned regions to have the same order and orientation in the two sequences.

Display of Alignments

For overviews of the alignment results, we used a visual representation called the percent identity plot (PIP) (Oeltjen et al. 1997; Hardison et al. 1997; Ansari-Lari et al. 1998). The PIPs, unlike the traditional representation of these alignments as dot-plots, lose some of the spatial relationships with one of the compared sequences but accurately depict the level of identity at each position in the alignment.

ACKNOWLEDGMENTS

We thank Victor Boyartchuk, James Watters, and Rebecca Mosher for critical evaluation of the manuscript and Jeremiah

Scharf and Lou Kunkel for helpful discussions. This work was supported by a grant from the Muscular Dystrophy Association to W.F.D., who is an assistant investigator of the Howard Hughes Medical Institute. W.M. was supported by grant LM05110 from the National Library of Medicine.

The publication costs of this article were defrayed in part by payment of page charges. This article must therefore be hereby marked "advertisement" in accordance with 18 USC section 1734 solely to indicate this fact.

REFERENCES

- Ansari-Lari, M.A., Oeltjen, J.C., Schwartz, S., Zhang, Z., Muzny, O.M., Lu, J., Gorrell, J.H., Chinault, A.C., Belmont, J.W., Miller, W., and Gibbs, R.A. 1998. Comparative sequence analysis of a gene-rich cluster at human chromosome 12p13 and its syntenic region in mouse chromosome 6. *Genome Res.* **8**: 29–40.
- Beckers, M.C., Yoshida, S., Morgan, K., Skamene, E., and Gros, P. 1995. Natural resistance to infection with *Legionella pneumophila*: Chromosomal localization of the *Lgn1* susceptibility gene. *Mamm. Gen.* **6**: 540–545.
- Burge, C. and Karlin, S. 1997. Prediction of complete gene structures in human genomic DNA. *J. Mol. Biol.* **268**: 78–94.
- Chen, E.Y., Schlessinger, D., and Kere, J. 1993. Ordered shotgun sequencing, a strategy for integrated mapping and sequencing of YAC clones. *Genomics* **17**: 651–656.
- Cheng, S., Fockler, C., Barnes, W., and Higuchi, R. 1994. Effective amplification of long targets from cloned inserts and human genomic DNA. *Proc. Natl. Acad. Sci.* **91**: 5695–5699.
- Dietrich, W.F., Damron, D.M., Isberg, R.R., Lander, E.S., and Swanson, M.S. 1995. *Lgn1*, a gene that determines susceptibility to *Legionella pneumophila*, maps to mouse chromosome 13. *Genomics* **26**: 443–450.
- Diez, E., Beckers, M.C., Ernst, E., DiDonato, C.J., Simard, L.R., Morissette, C., Gervais, F., Yoshida, S.I., and Gros, P. 1997. Genetic and physical mapping of the mouse host resistance locus *Lgn1*. *Mamm. Gen.* **8**: 682–685.
- Diez, E., Yaraghi, Z., MacKenzie, A., and Gros, P. 2000. The Neuronal Apoptosis Inhibitory Protein (Naip) is expressed in macrophages and is modulated after phagocytosis and during intracellular infection with *Legionella pneumophila*. *J. Immunol.* **164**: 1470–1477.
- Endrizzi, M., Huang, S., Scharf, J.M., Kelter, A.-R., Wirth, B., Kunkel, L.M., Miller, W., and Dietrich, W.F. 1999. Comparative Sequence Analysis of the Mouse and Human *Lgn1*/SMA interval. *Genomics* **60**: 137–151.
- Fritsch, E.F., Lawn, R.M., and Maniatis, T. 1980. Molecular cloning and characterization of the human beta-like globin gene cluster. *Cell* **19**: 959–972.
- Growney, J.D., and Dietrich, W.F. 2000. High resolution genetic and physical map of the *Lgn1* interval in C57BL/6j implicates *Naip2* or *Naip5* in *Legionella pneumophila* pathogenesis. *Genome Res.* This issue.
- Growney, J.D., Scharf, J.M., Kunkel, L.M., and Dietrich, W.F. 2000. Evolutionary divergence of the mouse and human *Lgn1*/SMA repeat structures. *Genomics* **64**: 62–81.
- Hardies, S.C., Edgell, M.H., and Hutchison, C.A. 1984. Evolution of the mammalian beta-globin gene cluster. *J. Biol. Chem.* **259**: 3748–3756.
- Hardison, R.C., Oeltjen, J., and Miller, W. 1997. Long human-mouse sequence alignments reveal novel regulatory elements: A reason to sequence the mouse genome. *Genome Res.* **7**: 959–966.
- Harris, N.L. 1997. Genotator: A workbench for sequence annotation. *Genome Res.* **7**: 754–762.
- Huang, S., Scharf, J.M., Growney, J.D., Endrizzi, M.G., and Dietrich, W.F. 1999. The mouse *Naip* gene cluster on Chromosome 13 encodes several distinct functional transcripts. *Mamm. Gen.* **10**: 1032–1035.
- Holcik, M., Thompson, C.S., Yaraghi, Z., Lefebvre, C.A., MacKenzie, A.E., and Korneluk, R.G. 2000. The hippocampal neurons of neuronal apoptosis inhibitory protein 1 (NAIP1)-deleted mice display increased vulnerability to kainic acid-induced injury. *Proc. Natl. Acad. Sci.* **97**: 2286–2290.
- Kulp, D., Haussler, D., Reese, M.G., and Eeckman, F.H. 1996. A generalized hidden marker mode for the recognition of human genes in DNA. *Proc. Intelligent Syst. Mol. Biol.* **4**: 134–142.
- Lefebvre, S., Burglen, L., Reboullet, S., Clermont, O., Burlet, P., Viollet, L., Benichou, B., Cruaud, C., Millasseau, P., Zeviani, M. et al. 1995. Identification and characterization of a spinal muscular atrophy-determining gene. *Cell* **80**: 155–165.
- Lincoln, S., Daly, M., and Lander, E.S. 1991. Whitehead Institute for Biomedical Research <http://www.genome.wi.mit.edu>.
- Nath, K., and Bollon, A.P. 1977. Organization of the yeast ribosomal RNA gene cluster via cloning and restriction analysis. *J. Biol. Chem.* **252**: 6562–6571.
- Nathans, J., Piantanida, T.P., Eddy, R.L., Shows, T.B., and Hogness, D.S. 1986. Molecular genetics of inherited variation in human color vision. *Science* **232**: 203–210.
- Oeltjen, J.C., Malley, T.M., Muzny, D.M., Miller, W., Gibbs, R.A., and Belmont, J.W. 1997. Large-scale comparative sequence analysis of the human and murine Bruton's tyrosine kinase loci reveals conserved regulatory domains. *Genome Res.* **7**: 315–329.
- Raymond, M., Rose, E., Housman, D.E., and Gros, P. 1990. Physical mapping, amplification, and overexpression of the mouse *mdr* gene family in multidrug-resistant cells. *Mol. Cell. Biol.* **10**: 1642–1651.
- Roy, N., Mahadevan, M.S., McLean, M., Shutler, G., Yaraghi, Z., Farahani, R., Baird, S., Besner-Johnston, A., Lefebvre, C., Kang, X. et al. 1995. The gene for neuronal apoptosis inhibitory protein is partially deleted in individuals with spinal muscular atrophy. *Cell* **80**: 167–178.
- Scharf, J.M., Damron, D., Frisella, A., Bruno, S., Beggs, A.H., Kunkel, L.M., and Dietrich, W.F. 1996. The mouse region syntenic for human spinal muscular atrophy lies within the *Lgn1* critical interval and contains multiple copies of *Naip* exon 5. *Genomics* **38**: 405–417.
- Schwartz, S., Zhang, Z., Fraser, K.A., Smit, A., Riemer, C., Bouck, J., Gibbs, R., Hardison, R., and Miller, W. 2000. PipMaker-A web server for aligning two genomic DNA sequences. *Genome Res.* **10**: 577–586.
- Solovyev, V.V., Salamov, A.A., and Lawrence, C.B. 1994. Predicting internal exons by oligonucleotide composition and discriminant analysis of spliceable open reading frames. *Nucleic Acids Res.* **22**: 5156–5163.
- Staden, R. 1996. The Staden sequence analysis package. *Mol. Biotechnol.* **5**: 233–241.
- Uberbacher, E.C. and Mural, R.J. 1991. Locating protein-coding regions in human DNA sequences by a multiple sensor-neural network approach. *Proc. Natl. Acad. Sci. USA.* **88**: 11261–11265.
- Yamamoto, Y., Klein, T.W., Newton, C.A., Widen, R., and Friedman, H. 1988. Growth of *Legionella pneumophila* in thioglycollate-elicited peritoneal macrophages from A/J mice. *Infect. Immun.* **56**: 370–375.
- Yamamoto, Y., Klein, T.W., and Friedman, H. 1991. *Legionella pneumophila* growth in macrophages from susceptible mice is genetically controlled. *Proc. Exp. Biol. Med.* **196**: 405–409.
- Yaraghi, Z., Korneluk, R.G., and MacKenzie, A. 1998. Cloning and characterization of the multiple murine homologs of NAIP (neuronal apoptosis inhibitory protein). *Genomics* **51**: 107–113.
- Yokoyama, S., Starmer, W.T., and Yokoyama, R. 1993. Paralogous origin of the red- and green-sensitive visual pigment genes in vertebrates. *Mol. Biol. Evol.* **10**: 527–538.
- Yoshida, S.I., Goto, Y., Mizuguchi, Y., Nomoto, K., and Skamene, E. 1991. Genetic control of natural resistance in mouse macrophages regulating intracellular *Legionella pneumophila* multiplication *in vitro*. *Infect. and Imm.* **59**: 428–432.

Received March 15, 2000; accepted in revised form June 2, 2000.